From particle methods to forward-backward Lagrangian schemes

Martin Campos Pinto, Frédérique Charles

HAL preprint, February 22, 2017

From particle methods to forward-backward Lagrangian schemes

Martin Campos Pinto [1]
Frédérique Charles [2]

[1] CNRS, Sorbonne Universités, UPMC Univ Paris 06, UMR 7598, Laboratoire Jacques-Louis Lions, 4, place Jussieu 75005, Paris, France
E-mail address: campos@ljll.math.upmc.fr
[2] Sorbonne Universités, UPMC Univ Paris 06, CNRS, UMR 7598, Laboratoire Jacques-Louis Lions, 4, place Jussieu 75005, Paris, France
E-mail address: charles@ljll.math.upmc.fr.

Abstract. In this article we study a novel method for improving the accuracy of density reconstructions based on markers pushed forward by some available particle code. The method relies on the backward Lagrangian representation of the transported density, and it evaluates the backward flow using the current position of point particles seen as flow markers. Compared to existing smooth particle methods with either fixed or transformed shapes, the proposed reconstruction achieves higher locality and accuracy. This is confirmed by our error analysis which shows a theoretical gain of one convergence order compared to the LTP/QTP methods introduced in [8], and by numerical experiments that demonstrate significative CPU gains and an improved robustness relative to the remapping period.

1. Introduction

Particle methods are a popular and efficient tool for the approximation of transport problems. Unfortunately they suffer from weak convergence properties which often prevent an accurate representation of the transported density.

To formalize the problem we consider an abstract transport equation

$$\partial_t f(t,x) + u(t,x)\cdot\nabla f(t,x) = 0, \qquad t\in[0,T], \quad x\in\mathbb{R}^d \tag{1.1}$$

associated with an initial data $f^0:\mathbb{R}^d\to\mathbb{R}$, a final time T and a velocity field $u:[0,T]\times\mathbb{R}^d\to\mathbb{R}^d$. In most cases of interest, the velocity u depends on f through some self-consistent coupling and the problem is non-linear. Here we shall leave this issue aside and assume that u is given and smooth, e.g. $L^\infty(0,T;W^{1;\infty}(\mathbb{R}^d))$, [29], so that there exist characteristic trajectories $X(t)=X(t;s,x)$ solutions to

$$X'(t) = u(t,X(t)), \qquad X(s)=x \tag{1.2}$$

on $[0,T]$, for all $x\in\mathbb{R}^d$ and $s\in[0,T]$. The corresponding flow $F_{s,t}:x\mapsto X(t)$ is then invertible and satisfies $(F_{s,t})^{-1}=F_{t,s}$. In particular, the solution to (1.1) reads

$$f(t,x) = f^0((F_{0,t})^{-1}(x)) \qquad \text{for } \ t\in[0,T],\ x\in\mathbb{R}^d. \tag{1.3}$$

Specifically, as reliable particle solvers do exist for many specific problems, see e.g. [15, 6], we may place ourself in the situation where we are given an accurate solver to push forward arbitrary sets of markers along the forward flow. For simplicity we will assume that the computed flow is exact, and we consider particles centers initially arranged on a cartesian grid of resolution h,

$$x_k^0 = hk, \qquad k\in\mathbb{Z}^d. \tag{1.4}$$

Thus, at time $t^n=n\Delta t$, $n\in\mathbb{N}$, we have at our disposal an unstructured set of particles of the form

$$x_k^n = F_{\rm ex}^{0,n}(x_k^0), \qquad k\in\mathbb{Z}^d, \quad \text{with } F_{\rm ex}^{0,n}=F_{0,t^n}$$

and we consider the problem of designing an accurate representation of the transported density $f(t^n)$. In the standard approach [19, 3, 29], the initial density is first approximated by a weighted collection of smooth "shape functions" centered on the particle positions, of the form

$$f^0_{h,\varepsilon}(x) = \sum_{k\in\mathbb{Z}^d} w^0_k \varphi_\varepsilon(x - x^0_k). \tag{1.5}$$

Here $\varphi_\varepsilon(x) := \varepsilon^{-d}\varphi(\varepsilon^{-1}x)$ is a smooth function with compact support (such as a B-spline or some convolution kernel with vanishing moments [26]) and ε is a smoothing scale which may or may not coincide with h. The weights are defined so that $f^0_{h,\varepsilon}$ approximates f^0 in a measure sense, for instance with $w^0_k = h^d f^0(x^0_k)$, see [29, Sec. I.4], and they evolve according to the differential equation

$$w_k'(t) - (\nabla\cdot u)\left(t, F_{0,t}(x^0_k)\right) w_k(t) = 0, \qquad w_k(0) = w^0_k.$$

The smooth particle approximation to f^n is then given by

$$f^n_{h,\varepsilon}(x) = \sum_{k\in\mathbb{Z}^d} w^n_k \varphi_\varepsilon(x - x^n_k) \tag{1.6}$$

with $w^n_k = w_k(t^n)$. Provided some r-th order moment condition on the smoothing kernel φ, the classical error estimate [29, Th. I.5.1] reads

$$\|f(t^n) - f^n_{h,\varepsilon}\|_{L^q} \lesssim \varepsilon^r \|f^0\|_{W^{r,q}} + (h/\varepsilon)^m \|f^0\|_{W^{m,q}}, \quad 1 \le q \le \infty. \tag{1.7}$$

Here we have assumed $h \lesssim \varepsilon$ (meaning that $h \le C\varepsilon$ for some constant independent of the expressed quantities), and we have denoted

$$\|v\|_{W^{r,q}(\omega)} := \|v\|_{L^q(\omega)} + \sum_{s=1}^{r} |v|_{W^{s,q}(\omega)} \qquad |v|_{W^{r,q}(\omega)} := \max_i \Big\{ \sum_{l_1=1}^{d} \cdots \sum_{l_r=1}^{d} \|\partial_{l_1}\cdots\partial_{l_r} v_i\|_{L^q(\omega)} \Big\} \tag{1.8}$$

for functions in Sobolev spaces $W^{r,q}(\omega)$ with $\omega \subset \mathbb{R}^d$, an for conciseness we drop the domain when $\omega = \mathbb{R}^d$. For vectors it will be convenient to use the maximum norm $\|x\|_\infty := \max_i |x_i|$ and the associated $\|A\|_\infty := \max_i \sum_j |A_{i,j}|$ for matrices.

One can improve (1.7) by changing the initial weights w^0_k to yield better quadrature formulas [11], but in any case such kind of estimates show a weakness of the reconstruction (1.6), namely the need to set $\varepsilon \gg h$ as $\varepsilon, h \to 0$, to guarantee the strong convergence of the approximated densities. As this would lead to a computationally expensive overlapping of particles, in practice many particle codes implement limited values of ε that appear to suffice for the accuracy of the trajectories. In the case where the particles trajectories are exact, the theory indeed guarantees the weak convergence of the approximated densities, independent of ε. Thus in the codes the lack of a sufficient particle overlapping typically translates into strong oscillations in the numerical approximations.

To mitigate these oscillations many authors have proposed to use remapping techniques where new weighted particles are periodically computed to approximate the transported density (1.6). The resulting schemes are often referred to as forward semi-Lagrangian [17, 22, 27, 13, 16, 25] and they have shown improved convergence rates based essentially on the fact that the frequent reinitializations prevent the particles to become too irregularly distributed. However this has a cost. On the computational level, reinitializing the particles can be expensive and it may introduce numerical diffusion, which conflicts with the conservative essence of the particle method. Advanced techniques have been used to reduce this diffusion, such as high-order non-oscillatory remeshing schemes [25] or multiscale methods, see e.g. [4, 5, 32].

In this article we take a different route to compute non-oscillatory density reconstructions. Following a series of previous works [1, 8, 10, 9], we study a new lagrangian method that implements in the

framework of forward particle methods an improved locality principle proposed by Colombi and Alard in [12] to design highly accurate semi-lagrangian schemes.

The outline is as follows. In Section 2 we remind how transforming the smooth particle shapes to better follow the characteristic flow allows to reconstruct accurate approximations to the density, at the price of extended particle supports. In Section 3 we then present our new method, for which we provide a priori error estimates in Section 4, and numerical results in Section 5.

2. Accurate particle transport with LTP and QTP approximations

2.1. Using particle shapes with polynomial transformations

Following a natural idea investigated by several authors [21, 2, 11, 14, 1] who considered transforming the smooth particle shapes according to the local variations of the flow, a numerical method to improve the accuracy of the density reconstruction has been proposed and analysed in [8]. Again, the approximated density is obtained as a superposition of weighted particles (now with $\varepsilon = h$),

$$f_h^n(x) = \sum_{k\in\mathbb{Z}^d} w_k \varphi_{h,k}^n(x), \qquad x \in \mathbb{R}^d, \tag{2.1}$$

but here each particle shape $\varphi_{h,k}^n$ is transported from the initial one in (1.5) using a polynomial flow defined as a local expansion of the exact backward flow

$$B_{\mathrm{ex}}^{0,n} = (F_{0,t_n})^{-1}.$$

Thus, at the first order the method uses a linearization of $B_{\mathrm{ex}}^{0,n}$ around the k-th particle,

$$B_{h,k,(1)}^{0,n} : x \mapsto x_k^0 + D_k^n(x - x_k^n)$$

with D_k^n an approximation to the $(d \times d)$ Jacobian matrix

$$J_{B_{\mathrm{ex}}^{0,n}}(x_k^n) = \left(\partial_j (B_{\mathrm{ex}}^{0,n})_i(x_k^n)\right)_{1\le i,j\le d}, \tag{2.2}$$

that is computed from the current position of the neighboring particles $x_{k'}^n$, $|k'-k| \le 1$, as recalled in Appendix A. The particle shapes are then defined accordingly, as

$$\varphi_{h,k}^n(x) = \varphi_h(B_{h,k}^{0,n}(x) - x_k^0) = \varphi_h(D_k^n(x - x_k^n)) \tag{2.3}$$

which correspond to translating and linearly transforming the particle shapes to better represent the local shear and rotation parts of the flow.

At the second order the local expansion of the backward flow $B_{h,k,(2)}^{0,n}$ takes the form

$$\left(B_{h,k,(2)}^{0,n}(x)\right)_i = (x_k^0)_i + (D_k^n(x - x_k^n))_i + (x - x_k^n)^t Q_{k,i}^n (x - x_k^n)$$

with $Q_{k,i}^n$ an approximation to the $(d \times d)$ Hessian matrix of the i-th component of the backward flow,

$$H_{(B_{\mathrm{ex}}^{0,n})_i}(x_k^n) = \left(\partial_{j_1}\partial_{j_2}(B_{\mathrm{ex}}^{0,n})_i(x_k^n)\right)_{1\le j_1,j_2\le d}, \qquad 1 \le i \le d, \tag{2.4}$$

Again these matrices can be computed using only the current position of the neighboring particles, $x_{k'}^n$, $|k'-k| \le 1$, see Appendix B. The quadratically transported particle shapes are then defined with the same principle. However it is necessary to define an a priori support for these particles: because the quadratic mapping $x \mapsto B_{h,k,(2)}^{0,n}(x) - x_k^0$ may vanish far away from x_k^n, the simple expression $\varphi_h(B_{h,k,(2)}^{0,n}(x) - x_k^0)$ has a support that may contain some far away parts, which is obviously not desired since the quadratic expansion $B_{h,k,(2)}^{0,n} \approx B_{\mathrm{ex}}^{0,n}$ is only accurate close to x_k^n. For this reason it is necessary to restrict a-priori the support of the quadratically transformed particles. In [8] a specific choice has been made, which allows to prove second-order convergence estimates for the resulting

approximations. This approach results in a robust numerical method, and several L^∞ convergence estimates have been derived for the transported densities [8, 9]. However it also has the downside that transported particles undergo a stretching of their support which leads to an important loss in the locality of the computations. Specifically, we see that as time increases the diameter of the particle supports grows like

$$\operatorname{diam}\left(\operatorname{supp}(\varphi^n_{h,k})\right) = \operatorname{diam}\left(F^{0,n}_{\mathrm{ex}}(\operatorname{supp}(\varphi^0_{h,k}))\right) \sim h|F^{0,n}_{\mathrm{ex}}|_{W^{1,\infty}}$$

in the LTP case, which may represent an exponential growth in n. In the QTP method the supports grow even faster, to account for the additional deformations caused by the quadratic terms.

This effect has been experienced in the numerical simulations of high-dimensional problems such as the 2D2V Vlasov-Poisson system actually implemented in the Selalib platform [30], and it is already visible in the 2D simulations presented in this article, especially with second order methods.

2.2. **Notations**

Here we summarize the notations used in the article for the different flows and their derivatives:

$F^{0,n}_{\mathrm{ex}}$	:	exact forward flow on the time interval $[0, t^n]$
$B^{0,n}_{\mathrm{ex}}$	:	exact backward flow on the time interval $[0, t^n]$
$J_{B^{0,n}_{\mathrm{ex}}}(x^n_k)$	:	Jacobian matrix of $B^{0,n}_{\mathrm{ex}}$ evaluated at x^n_k, the position of the particle k at time t^n
$H_{(B^{0,n}_{\mathrm{ex}})_i}(x^n_k)$	:	Hessian matrix of the component i of $B^{0,n}_{\mathrm{ex}}$ at x^n_k
$B^{0,n}_{k,(1)}$	:	linear expansion of $B^{0,n}_{\mathrm{ex}}$ around x^n_k (using the exact flow derivatives)
$B^{0,n}_{k,(2)}$	:	quadratic expansion of $B^{0,n}_{\mathrm{ex}}$ around x^n_k (using the exact flow derivatives)
D^n_k	:	particle-based approximation of $J_{B^{0,n}_{\mathrm{ex}}}(x^n_k)$
$Q^n_{k,i}$	:	particle-based approximation of $H_{(B^{0,n}_{\mathrm{ex}})_i}(x^n_k)$
$B^{0,n}_{h,k,(1)}$	:	linear expansion of $B^{0,n}_{\mathrm{ex}}$ around x^n_k, using the matrix D^n_k
$B^{0,n}_{h,k,(2)}$	:	quadratic expansion of $B^{0,n}_{\mathrm{ex}}$ around x^n_k, using the matrices D^n_k and $Q^n_{k,i}$, $1 \le i \le d$
$B^{0,n}_h$	:	global approximation of $B^{0,n}_{\mathrm{ex}}$ used in the FBL reconstruction.

In the remapped version of the methods, the above notations will be extended to time intervals of the form $[t^m, t^n]$ with m the last remapping time step preceeding n (see, e.g. Section 3.2).

3. **The Forward-Backward Lagrangian (FBL) approximation**

Since it is the accurate transport of the smooth particle shapes that causes a loss of locality in the computation of the approximated density, a natural option to restore locality is to follow the elegant approach of [12] and abandon the forward description of f. We shall, however, recycle one central step of the method described above, and continue using the local approximations to the backward flow that can be computed locally from the current particle positions. Instead of computing directly an accurate approximation to f under the form of transported particles, we thus propose to combine a pointwise particle approximation of the flow with a backward Lagrangian approximation to f.

The resulting method combines a *forward* part where pointwise particles are pushed along a standard numerical flow, and a *backward* step where the transported density is reconstructed with a Lagrangian point of view thanks to a approximation of the backward flow.

3.1. **Description of the method**

The FBL approximation to the exact solution $f(t^n,x) = f^0(B_{\rm ex}^{0,n}(x))$ consists of the following steps.

(i) To every particle x_k^n we associate a polynomial backward flow $B_{h,k}^{0,n}$ which approximates the exact one close to x_k^n, as in the LTP and QTP methods. We remind that at the first order this flow reads

$$B_{h,k}^{0,n} = B_{h,k,(1)}^{0,n} : x \mapsto x_k^0 + D_k^n(x - x_k^n) \qquad \text{with} \quad D_k^n \approx J_{B_{\rm ex}^{0,n}}(x_k^n) \tag{3.1}$$

see Appendix A, and at the second order it takes the form

$$B_{h,k}^{0,n} = B_{h,k,(2)}^{0,n} : x \mapsto x_k^0 + D_k^n(x - x_k^n) + \frac{1}{2}\big((x - x_k^n)^t Q_{k,i}^n (x - x_k^n)\big)_{1\le i\le d} \tag{3.2}$$

with $Q_{k,i}^n \approx H_{(B_{\rm ex}^{0,n})_i}(x_k^n)$, $1 \le i \le d$, see Appendix B.

(ii) To smoothly patch these local flows together we then consider a partition of unity

$$\sum_{i\in\mathbb{Z}^d} S(x - i) = 1, \qquad x \in \mathbb{R}^d \tag{3.3}$$

involving a compactly supported, non-negative shape function S (for instance a B-spline), and a grid of step size h. Writing the corresponding nodes as $\xi_i = ih$ to avoid a confusion with the particle positions, the scaled formula reads $\sum_{i\in\mathbb{Z}^d} S_{h,i}(x) = 1$ where $S_{h,i}(x) = S\big((x - \xi_i)/h\big)$. A global approximation to the backward flow is then defined as

$$B_h^{0,n}(x) := \sum_{i\in\mathbb{Z}^d} B_{h,k^*(n,i)}^{0,n}(x) S_{h,i}(x) \tag{3.4}$$

where $k^*(n,i)$ is the index of the closest marker to the node ξ_i,

$$k^*(n,i) := \mathrm{argmin}_{k\in\mathbb{Z}^d} \|x_k^n - \xi_i\|_\infty.$$

(iii) The approximate solution is finally obtained by a standard Lagrangian formula involving the initial density

$$f_h^{n,\rm fbl}(x) := f^0\big(B_h^{0,n}(x)\big). \tag{3.5}$$

Remark 3.1 (conservative transport)**.** The FBL approximation can be extended with little extra cost to the case of a transport equation in conservation form

$$\partial_t f(t,x) + \nabla\cdot(uf)\,(t,x) = 0. \tag{3.6}$$

In the case of an incompressible flow ($\nabla\cdot u = 0$), this form is equivalent with (1.1). Otherwise the exact solution to (3.6) reads

$$f(t,x) = f^0((B_{\rm ex}^{0,n}(x))\det(J_{B_{\rm ex}^{0,n}}(x)).$$

Consistent with the spirit of the reconstruction (3.5), an approximation $j_h^{0,n}(x)$ to $\det(J_{B_{\rm ex}^{0,n}}(x))$ is defined by

$$j_{h,i}^{0,n} = \det(D_{k^*(n,i)}), \qquad j_h^{0,n}(x) = \sum_{i\in\mathbb{Z}^d} j_{h,i}^{0,n} S_{h,i}(x)$$

and we define the corresponding FBL approximation to the transported density by

$$j_h^{n,\rm fbl}(x) := f^0\big(B_h^{0,n}(x)\big) j_h^{0,n}(x). \tag{3.7}$$

3.2. **Remapped FBL method**

Because the regularity of the characteristic flow deteriorates over time, it is important to remap the particles before the approximated flow becomes too inaccurate. Remapping essentially consists of using the density transported up to some time t_m as the initial data of a new transport problem, so that the relevant flow map is reset to the identity. Specifically we replace the approximate density (3.5) given by the FBL method with a new nodal representation on the grid,

$$f_h^m(x) = \sum_k w_k^m \varphi_h(x - x_k^0) \approx f_h^{m,\mathrm{fbl}}(x) \tag{3.8}$$

and for the subsequent time steps we follow a new set of particles arranged on the cartesian grid (1.4).

To project on the grid we may use tensor products of univariate B-splines defined recursively by $\mathcal{B}_p(x) = \int_{x-\frac{1}{2}}^{x+\frac{1}{2}} \mathcal{B}_{p-1}$, $\mathcal{B}_0 := \chi_{[-\frac{1}{2},\frac{1}{2}]}$. The approximation reads then

$$A_h g(x) := \sum_{k\in\mathbb{Z}^d} a_{h,k}(g)\varphi_h(x - x_k^0), \qquad \varphi_h(x) = \prod_{1\le i\le d} \frac{1}{h}\mathcal{B}_p\left(\frac{x_i}{h}\right)$$

where $a_{h,k}(g)$ is a coefficient that depends on the values of g on a local stencil around x_k^0, such that polynomials of degree $\geq p$ are exactly reproduced by A_h, see [31, 8], but many other approximations are possible. Here we simply assume that A_h satisfies

$$\|A_h g - g\|_{W^{s,\infty}} \le C_A h^{q-s} |g|_{W^{q,\infty}}, \qquad \text{for } 0 \le s \le q \le p+1 \tag{3.9}$$

for some constant c_A.

Thus, if we denote the remapping steps by $m_1, \dots m_R$ and let $m_0 = 0$ be the initial step where the initial data f^0 is also projected, the remapped-FBL approximation reads

$$f_h^{n,\mathrm{fbl}}(x) = f_h^m\big(B_h^{m,n}(x)\big), \qquad m = \max\big\{m_r < n : r \in \{0,\dots,R\}\big\} \tag{3.10}$$

with

- a numerical flow
$$B_h^{m,n} = \sum_{i\in\mathbb{Z}^d} B_{h,k^*(n,i)}^{m,n} S_{h,i} \tag{3.11}$$
computed with the FBL method (3.4), using the current particles $x_k^n = F_{\mathrm{ex}}^{m,n}(x_k^0)$,

- a numerical density f_h^m which is either the approximation of the initial data, or that of an approximated solution transported with the FBL method if m is a remapping step, that is,
$$f_h^m = \begin{cases} A_h f^0 & \text{if } m = m_0 = 0 \\ A_h f_h^{m,\mathrm{fbl}} & \text{if } m = m_r > 0. \end{cases} \tag{3.12}$$

We note that if we only consider the remapping time steps the proposed method is formally a backward semi-Lagrangian scheme

$$f_h^{m_{r+1}} = A_h\Big(f_h^{m_r} \circ B_h^{m_r,m_{r+1}}\Big) \tag{3.13}$$

where the approximated backward flow is computed using the forward-pushed markers.

4. A priori error analysis

Following the error analysis established in [8] for the LTP and QTP methods, it is possible to derive a priori convergence rates for the proposed method. Here we take into account the error induced by the particle-based approximation of the Jacobian matrices, and estimates are available provided h is small enough to guarantee that these matrices are invertible, see Appendix. We first consider the case where no remappings are performed.

4.1. A priori estimates for the FBL method without remappings

Theorem 4.1. *Let $h \le h^*(F^{0,n}_{\rm ex})$ as in* (A.6) *and assume $B^{0,n}_{\rm ex}$ and $F^{0,n}_{\rm ex} \in W^{2,\infty}(\mathbb{R}^d)$. The first order FBL approximation* (3.5) *satisfies*

$$\|f_h^{n,\rm fbl} - f(t^n)\| \le Ch^2$$

with a constant independent of h that is specified in the proof.

Remark 4.2. Compared to the a priori error estimates established for the LTP method [8], this result represents a gain of one order.

Proof. By direct application of a Taylor expansion we see that the (exact) linearization of the backward flow around some particle x^n_k, namely

$$B^{0,n}_{k,(1)} : x \mapsto x^0_k + \big(J_{B^{0,n}_{\rm ex}(x^n_k)}\big)(x - x^n_k)$$

satisfies an priori estimate

$$\|B^{0,n}_{k,(1)}(x) - B^{0,n}_{\rm ex}(x)\|_\infty \le \frac{1}{2}|B^{0,n}_{\rm ex}|_{W^{2,\infty}}\|x - x^n_k\|^2_\infty. \tag{4.1}$$

Thanks to the assumption $h \le h^*(F^{0,n}_{\rm ex})$ we can next use Lemma A.1 (specifically, estimate (A.7) with $q = 1$) to estimate the FD approximation on the backward flow Jacobian matrix. For the local numerical flow (3.1), we thus have

$$\begin{aligned}\|B^{0,n}_{h,k,(1)}(x) - B^{0,n}_{\rm ex}(x)\|_\infty &\le \|(D^n_k - J_{B^{0,n}_{\rm ex}(x^n_k)})(x - x^n_k)\|_\infty + \|B^{0,n}_{k,(1)}(x) - B^{0,n}_{\rm ex}(x)\|_\infty \\ &\le C_F\|x - x^n_k\|_\infty\Big(d^2|F^{0,n}_{\rm ex}|_1^{2(d-1)}h + \frac{1}{2}\|x - x^n_k\|_\infty\Big)\end{aligned} \tag{4.2}$$

with $C_F = \max\big(|B^{0,n}_{\rm ex}|_{W^{2,\infty}}, |F^{0,n}_{\rm ex}|_{W^{2,\infty}}\big)$. Our estimate for the global flow $B^{0,n}_h$ will gather bounds of this form for $k = k^*(n,i)$ with $i \in \mathbb{Z}^d$, and $x \in \mathrm{supp}(S_{h,i})$ where $S_{h,i}(x) := S\left(\frac{1}{h}(x - \xi_i)\right)$. In particular, we need to evaluate the distance between a node ξ_i and its associated particle $x^n_{k^*(n,i)}$, and to this end we note that for an arbitrary $k \in \mathbb{Z}^d$ we have

$$\|x^n_k - \xi_i\|_\infty = \|F^{0,n}_{\rm ex}(x^0_k) - F^{0,n}_{\rm ex}(B^{0,n}_{\rm ex}(\xi_i))\|_\infty \le |F^{0,n}_{\rm ex}|_{W^{1,\infty}}\|x^0_k - B^{0,n}_{\rm ex}(\xi_i)\|_\infty.$$

By definition of $k^*(n,i)$ and using the fact that the markers x^0_k are on a grid of step h, this yields

$$\|x^n_{k^*(n,i)} - \xi_i\|_\infty \le |F^{0,n}_{\rm ex}|_{W^{1,\infty}} \min_{k\in\mathbb{Z}^d}\|x^0_k - B^{0,n}_{\rm ex}(\xi_i)\|_\infty \le \frac{h}{2}|F^{0,n}_{\rm ex}|_{W^{1,\infty}}.$$

Writing then $\rho_S = \frac{1}{2}\,\mathrm{diam}(\mathrm{supp}(S))$ we see that the support of $S_{h,i}$ is an ℓ^∞ ball of center ξ_i and radius $h\rho_S$. Thus,

$$x \in \mathrm{supp}(S_{h,i}) \quad \Longrightarrow \quad \|x - x^n_{k^*(n,i)}\|_\infty \le \|x - \xi_i\|_\infty + \|\xi_i - x^n_{k^*(n,i)}\|_\infty \le h\rho(S,n)$$

with

$$\rho(S,n) := \rho_S + \frac{1}{2}|F^{0,n}_{\rm ex}|_{W^{1,\infty}}. \tag{4.3}$$

In particular, the bound (4.2) evaluated for $k = k^*(n,i)$ gives

$$\|B^{0,n}_{h,k^*(n,i),(1)} - B^{0,n}_{\rm ex}\|_{L^\infty(\mathrm{supp}(S_{h,i}))} \le C_1h^2, \qquad i \in \mathbb{Z}^d \tag{4.4}$$

with

$$C_1 = C_F \rho(S,n)\big(d^2 |F_{\rm ex}^{0,n}|_1^{2(d-1)} + \frac{1}{2}\rho(S,n)\big). \tag{4.5}$$

Using the partition unity properties of the shape function S, we then write for the global flow

$$(B_h^{0,n} - B_{\rm ex}^{0,n})(x) = \sum_{i\in\mathbb{Z}^d} (B^{0,n}_{h,k^*(n,i),(1)} - B_{\rm ex}^{0,n})(x) S_{h,i}(x) \le C_1 h^2 \sum_{i\in\mathbb{Z}^d} S_{h,i}(x) = C_1 h^2, \qquad x\in\mathbb{R}^d. \tag{4.6}$$

Using the smoothness of f^0 completes the proof, with $C = C_1 |f^0|_{W^{1,\infty}}$. ∎

Theorem 4.3. *Let $h \le h^*(F_{\rm ex}^{0,n})$ as in* (A.6) *and assume $B_{\rm ex}^{0,n}$ and $F_{\rm ex}^{0,n} \in W^{3,\infty}(\mathbb{R}^d)$. The second order FBL approximation* (3.5) *satisfies*

$$\|f_h^{n,\rm fbl} - f(t^n)\| \le C h^3$$

with a constant that depends on the exact flow $F_{\rm ex}^{0,n}$ and its inverse $B_{\rm ex}^{0,n}$, but is independent of h.

Remark 4.4. Compared to the error estimates established for the QTP method [8], this result represents a gain of one order. Moreover this scheme is simpler as it does not require to estimate a priori supports for transformed particles.

Proof. The proof is similar to that of Theorem 4.3. Applying a Taylor expansion we first observe that the (exact) quadratic approximation of the backward flow around some particle x_k^n, namely

$$B_{k,(2)}^{0,n} : x \mapsto x_k^0 + \big(J_{B_{\rm ex}^{0,n}}(x_k^n)\big)(x - x_k^n) + \frac{1}{2}\big((x-x_k^n)^t \big(H_{(B_{\rm ex}^{0,n})_i}(x_k^n)\big)(x-x_k^n)\big)_{1\le i\le d}$$

satisfies an priori estimate

$$\|B_{k,(2)}^{0,n}(x) - B_{\rm ex}^{0,n}(x)\|_\infty \le \frac{1}{6} |B_{\rm ex}^{0,n}|_{W^{3,\infty}} \|x - x_k^n\|_\infty^3. \tag{4.7}$$

Thanks to the assumption $h \le h^*(F_{\rm ex}^{0,n})$ we can next use Lemma A.1 (specifically, estimate (A.7) with $q=2$) and B.1 to estimate the FD approximations for the backward flow Jacobian and Hessian matrices. For the local numerical flow (3.2), we thus have

$$\begin{aligned}\|B_{h,k,(2)}^{0,n}(x) - B_{\rm ex}^{0,n}(x)\|_\infty &\le \|B_{k,(2)}^{0,n}(x) - B_{\rm ex}^{0,n}(x)\|_\infty + \|D_k^n - J_{B_{\rm ex}^{0,n}}(x_k^n)\|_\infty \|(x-x_k^n)\|_\infty \\ &\qquad + C \max_i \|Q_{k,i}^n - H_{(B_{\rm ex}^{0,n})_i}(x_k^n)\|_\infty \|(x-x_k^n)\|_\infty^2 \qquad (4.8)\\ &\le C(F_{\rm ex}^{0,n})\big(\|x-x_k^n\|_\infty^3 + h\|x-x_k^n\|_\infty^2 + \|x-x_k^n\|_\infty h^2\big)\end{aligned}$$

with a constant depending on the exact flow. The rest of the proof is the same. ∎

Remark 4.5. In the case of the FBL approximation (3.7) of the conservative transport equation, it is possible to prove using the same arguments that if $B_{\rm ex}^{0,n}$ and $F_{\rm ex}^{0,n} \in W^{3,\infty}(\mathbb{R}^d)$ then the first order FBL approximation (3.5) satisfies, under a modified condition on h which could writes $h \le h^{**}(F_{\rm ex}^{0,n})$,

$$\|g_h^{n,\rm fbl} - g(t^n)\| \le C h^2$$

with a constant independent of h.

4.2. **A priori estimates for the FBL method with remappings**

Let us denote by $\|A\|_{L^\infty} = \inf_{g\in\mathcal{C}} \frac{\|A_h g\|_{L^\infty}}{\|g\|_{L^\infty}}$ the L^∞ norm of the approximation operator A_h. We have the following estimate for the remapped method described in Section 3.2.

Theorem 4.6. *Assume that f^0, $F_{\rm ex}^{0,n}$ and $B_{\rm ex}^{0,n} \in W^{2,\infty}(\mathbb{R}^d)$. If the remapping time steps are such that $h \le h^*(F^{m_{r-1},m_r})$ for $r = 1,\dots,R$, as in* (A.6)*, then the (first order) remapped FBL scheme* (3.10)-(3.12) *satisfies*

$$\|f_h^{n,\rm fbl} - f(t^n)\| \le Ch^2 \tag{4.9}$$

with a constant specified in the proof, that may depend on the number of remappings R but not on h.

Proof. Writing m the last remapping step before n, the remapped FBL approximation reads $f_h^{n,\rm fbl}(x) = f_h^m(B_h^{m,n}(x))$, whereas the exact solution $f^n = f(t^n)$ satisfies $f^n(x) = f^m(B_{\rm ex}^{m,n}(x))$. Thus, we have

$$\begin{aligned}\|f_h^{n,\rm fbl} - f^n\|_{L^\infty} &\le \|f_h^m(B_h^{m,n}) - f^m(B_h^{m,n})\|_{L^\infty} + \|f^m(B_h^{m,n}) - f^m(B_{\rm ex}^{m,n})\|_{L^\infty}\\ &\le \|f_h^m - f^m\|_{L^\infty} + |f^m|_{W^{1,\infty}}\|B_h^{m,n} - B_{\rm ex}^{m,n}\|_{L^\infty}.\end{aligned} \tag{4.10}$$

Since the flow $B_h^{m,n}$ is obtained by applying the FBL method on the particles transported from t_m to t_n, the arguments used above to establish the bound (4.6) give here

$$\|B_h^{m,n} - B_{\rm ex}^{m,n}\|_{L^\infty} \le C_{m,n}h^2$$

with $C_{m,n} = |F^{m,n}|_{W^{2,\infty}}\rho(S,n-m)\big(d^2|F_{\rm ex}^{m,n}|_1^{2(d-1)} + \frac{1}{2}\rho(S,n-m)\big)$ and $\rho(S,\cdot)$ is defined in (4.3). As for the remapped approximation error at time t_m, it satisfies

$$\begin{aligned}\|f_h^m - f^m\|_{L^\infty} &\le \|A_h(f_h^{m,\rm fbl} - f^m)\|_{L^\infty} + \|(A_h - I)f^m\|_{L^\infty}\\ &\le \|A_h\|_{L^\infty}\|f_h^{m,\rm fbl} - f^m\|_{L^\infty} + C_A|f^m|_{W^{2,\infty}}h^2.\end{aligned}$$

Gathering the above estimates thus yields

$$\|f_h^{n,\rm fbl} - f^n\|_{L^\infty} \le \|A_h\|_{L^\infty}\|f_h^{m,\rm fbl} - f^m\|_{L^\infty} + h^2\Big(C_A|f^m|_{W^{2,\infty}} + C_{m,n}|f^m|_{W^{1,\infty}}\Big).$$

Denoting for convenience by $m_{R+1} = N$ the last time step (where no remapping is actually performed) we then observe that the error term defined by $e_r := \max_{m_{r-1}<n\le m_r}\|f_h^{n,\rm fbl} - f^n\|_{L^\infty}$ for $r \ge 1$ and $e_0 := 0$ satisfies a recursive bound

$$e_r \le \|A_h\|_{L^\infty}e_{r-1} + \beta h^2, \qquad r = 1,\dots R+1,$$

where we have denoted

$$\beta = C_A\|f\|_{L^\infty([0,T];W^{2,\infty})} + \max_{1\le r\le R+1}\ \max_{m_{r-1}<n\le m_r}\big(|f^{m_{r-1}}|_{W^{1,\infty}}C_{m_{r-1},n}\big).$$

This gives $e_r \le \alpha_r\beta h^2$ with $\alpha_r = (\|A_h\|_{L^\infty}^r - 1)/(\|A_h\|_{L^\infty} - 1)$ if $\|A_h\|_{L^\infty} > 1$ and $\alpha_r = r$ if $\|A_h\|_{L^\infty} = 1$. In particular this implies

$$\|f_h^{n,\rm fbl} - f^n\|_{L^\infty} \le \alpha_{R+1}\beta h^2$$

for all $n \le N = m_{R+1}$, which ends the proof. ∎

Remark 4.7. For stable approximation operators (such as piecewise affine interpolations) we have $\|A\|_{L^\infty} = 1$ and the constant C in (4.9) depends linearly of the number of remappings. In any case, this number should not vary much with h when the latter is small, indeed the remapping frequency should essentially reflect the smoothness of the exact characteristic flow.

4.3. **Transport of smoothness**

In the above analysis we did not take advantage of the fact that the reconstructed flow was obtained with a smooth patching procedure (3.4). Nevertheless, this feature of the FBL method allows to estimate the smoothness of the transported solutions as time evolves, and this may yield enhanced error bounds in the remapped version of the scheme, since remapping errors strongly depend on the solution smoothness. We illustrate this property with the following result.

Theorem 4.8. *The density transported with the FBL scheme* (3.5) *of order* $r \in \{1,2\}$ *satisfies*

$$\|f_h^{n,\mathrm{fbl}}\|_{W^{q,\infty}} \leq C\|f^0\|_{W^{q,\infty}}, \qquad 1 \leq q \leq r+1,$$

with a constant C *that depends on the exact flow* $F_{\mathrm{ex}}^{0,n}$ *and its inverse* $B_{\mathrm{ex}}^{0,n}$*, but not on* h*.*

Proof. We only give the proof in the case of the first order method ($r=1$), as that of the second order is similar. By differentiating the transported density $f_h^{n,\mathrm{fbl}} = f^0(B_h^{0,n})$ one obtains

$$\partial_j f_h^{n,\mathrm{fbl}}(x) = \sum_{l=1}^{d} \partial_l f^0(B_h^{0,n}(x))\partial_j (B_h^{0,n})_l(x), \qquad 1 \leq j \leq d,$$

and

$$\partial_{j_2}\partial_{j_1} f_h^{n,\mathrm{fbl}}(x) = \sum_{l_1,l_2=1}^{d} \partial_{l_2}\partial_{l_1} f^0(B_h^{0,n}(x))\partial_{j_1}\big(B_h^{0,n}\big)_{l_1}(x)\partial_{j_2}\big(B_h^{0,n}\big)_{l_2}(x)$$
$$+ \sum_{l=1}^{d} \partial_l f^0(B_h^{0,n}(x))\partial_{j_2}\partial_{j_1}\big(B_h^{0,n}\big)_l(x), \qquad 1 \leq j_1, j_2 \leq d.$$

This yields

$$|f_h^{n,\mathrm{fbl}}|_{W^{1,\infty}} \leq C|B_h^{0,n}|_{W^{1,\infty}}|f^0|_{W^{1,\infty}}$$

and

$$|f_h^{n,\mathrm{fbl}}|_{W^{2,\infty}} \leq C\big(|B_h^{0,n}|^2_{W^{1,\infty}}|f^0|_{W^{2,\infty}} + |B_h^{0,n}|_{W^{2,\infty}}|f^0|_{W^{1,\infty}}\big)$$

with constants depending only on d. We are then left to estimate the smoothness of the reconstructed flow $B_h^{0,n} = \sum_{i\in\mathbb{Z}^d} B_{h,k^*(n,i)}^{0,n} S_{h,i}$, which partial derivative reads

$$\partial_j\big(B_h^{0,n}\big)_l = \sum_{i\in\mathbb{Z}^d} \Big(\partial_j\Big(B_{h,k^*(n,i)}^{0,n}\Big)_l S_{h,i} + \Big(B_{h,k^*(n,i)}^{0,n}\Big)_l \partial_j S_{h,i}\Big). \tag{4.11}$$

Here the first term is easily taken care of by using the fact that the Jacobian matrix of the local affine flow $B_{h,k}^{0,n}$ is the matrix D_k^n, see (3.1), for which an a priori bound is given in the Appendix, see (A.13). Bounding the second term is less obvious since an $1/h$ factor appears in the derivative of $S_{h,i}(x) = S((x-\xi)/h)$. To handle this term we then observe that the sum $\sum_{i\in\mathbb{Z}^d}\partial_j S_{h,i}$ vanishes, thanks to the unity partition property (3.3). Hence we can write, for all $x \in \mathbb{R}^d$,

$$\Big|\sum_{i\in\mathbb{Z}^d}\Big(B_{h,k^*(n,i)}^{0,n}\Big)_l \partial_j S_{h,i}\Big|(x) = \Big|\sum_{i\in\mathbb{Z}^d}\Big(B_{h,k^*(n,i)}^{0,n} - B_{\mathrm{ex}}^{0,n}\Big)_l \partial_j S_{h,i}\Big|(x)$$
$$\leq \sum_{i\in\mathbb{Z}^d} \|B_{h,k^*(n,i)}^{0,n} - B_{\mathrm{ex}}^{0,n}\|_{L^\infty(\mathrm{supp}(S_{h,i}))}|\partial_j S_{h,i}|(x) \leq Ch$$

where we have used the local flow error estimate (4.4) and the bounded overlapping of the shapes $S_{h,i}$ (here the constant depends on the shape S and the flow $F_{\mathrm{ex}}^{0,n}$). This allows us to bound the first derivatives of $B_h^{0,n}$,

$$|B_h^{0,n}|_{W^{1,\infty}} \leq C(F_{\mathrm{ex}}^{0,n}).$$

For the second derivatives we proceed similarly. Differentiating (4.11) and using the affine nature of the local flows, we write

$$\partial_{j_2}\partial_{j_1}\big(B_h^{0,n}\big)_l = \sum_{i\in\mathbb{Z}^d}\Big(\partial_{j_1}\Big(B_{h,k^*(n,i)}^{0,n}\Big)_l \partial_{j_2} S_{h,i} + \partial_{j_2}\Big(B_{h,k^*(n,i)}^{0,n}\Big)_l \partial_{j_1} S_{h,i} + \Big(B_{h,k^*(n,i)}^{0,n}\Big)_l \partial_{j_2}\partial_{j_1} S_{h,i}\Big).$$

Again we can use the above trick and replace the local flows by local flow errors. In the last term the estimate (4.4) gives an h^2 factor that allows to take care of the $1/h^2$ term coming from the second derivatives of the scaled shape $S_{h,i}$, and in the derivatives we are lead to in considering the local error

on the backward Jacobian matrix, namely $D^n_{k^*(n,i)} - J_{B^{0,n}}(x)$ for $x \in \mathrm{supp}(S_{h,i})$, which is shown to be controlled by Ch by reasonning just as in the proof of Theorem 4.1. Thus, we finally have that

$$|B^{0,n}_h|_{W^{2,\infty}} \leq C$$

which completes the proof for the first-order method. The case of the second-order FBL method is completely similar, using the fact that the local flow errors are estimated with one higher order of accuracy in the proof of Theorem 4.3. ∎

5. **Numerical results**

In previous works [8, 10] the performances of the LTP and QTP schemes have been assessed by comparing them with existing methods such as standard smooth particle reconstructions (1.6) or, in the case of a non-linear Vlasov-Poisson problem, with modern semi-Lagrangian schemes.

Here we investigate the numerical efficiency of the proposed FBL approximation by comparing it with the LTP and QTP method, using either passive problems with given velocity fields, or non-linear transport problems.

5.1. **Passive transport problems**

As in [8] we consider several passive transport problems in 2d. The corresponding velocity fields are

- the reversible "swirling" velocity field proposed by LeVeque [24] to study the accuracy of high-resolution schemes for multidimensional advection problems,

$$u_{\mathrm{SW}}(t,x;T) := \cos\Big(\frac{\pi t}{T}\Big)\,\mathrm{curl}\,\phi_{\mathrm{SW}}(x) \quad \text{with} \quad \phi_{\mathrm{SW}}(x) := -\frac{\sin^2(\pi x_1)\sin^2(\pi x_2)}{\pi}$$

- another reversible velocity field emulating a Raylegh-Benard convection cell,

$$u_{\mathrm{RB}}(t,x;T) := \cos\Big(\frac{\pi t}{T}\Big)\,\mathrm{curl}\,\phi_{\mathrm{RB}}(x)$$

  with $\phi_{\mathrm{RB}}(x) := \big(x_1 - \frac{1}{2}\big)(x_1 - x_1^2)(x_2 - x_2^2)$;

- and finally a constant non-linear rotation field derived from Example 2 in [7],

$$u_{\mathrm{NLR}}(x) := \alpha(x)\begin{pmatrix}\frac{1}{2} - x_2\\ x_1 - \frac{1}{2}\end{pmatrix} \quad \text{with} \quad \alpha(x) := \Big(1 - \frac{\|x - (\frac{1}{2},\frac{1}{2})\|_2}{0.4}\Big)^3_+.$$

Here the form of u_{SW} and u_{RB} yields reversible problems: at $t = T/2$ the solutions reach a maximum stretching, and they revert to their initial value at $t = T$. As for the non-linear rotation field u_{NLR}, it is associated with the exact backward flow

$$B^{0,n}(x) = \begin{pmatrix}\frac{1}{2}\\ \frac{1}{2}\end{pmatrix} + \begin{pmatrix}\cos(\alpha(x)t^n) & \sin(\alpha(x)t^n)\\ -\sin(\alpha(x)t^n) & \cos(\alpha(x)t^n)\end{pmatrix}\begin{pmatrix}x_1 - \frac{1}{2}\\ x_2 - \frac{1}{2}\end{pmatrix}, \tag{5.1}$$

and the exact solutions are given by $f(t^n,x) = f^0(B^{0,n}(x))$. In addition to the above velocity fields we consider the following initial data:

- smooth humps of approximate radius 0.2 given by

$$f^0_{\mathrm{hump}}(x;\bar{x}) := \frac{1}{2}\Big(1 + \mathrm{erf}\Big(\tfrac{1}{3}(11 - 100\|x - \bar{x}\|_2)\Big)\Big)$$

  and centered on $\bar{x} = (0.5, 0.4)$ or $(0.5, 0.7)$, depending on the cases ;

- and for the non-linear rotation field u_{NLR} we take an initial data corresponding to Example 2 from [7], i.e.,
$$f^0(x) := x_2 - \tfrac{1}{2}.$$

By combining the above values we obtain the three test-cases in Table 1, and accurate solutions are shown in Figures 1-3 for the purpose of illustration. In Table 1 we also give the respective time steps Δt used in the time integration of the particle trajectories. In every case indeed, the numerical flow F^n is computed with a RK4 scheme, and the time steps have been taken small enough to have no significant effect on the final accuracy. It happens that in every case we have $\Delta t = T/100$, but this is unintended.

Table 1. Definition of the benchmark test-cases

name	$u(t,x)$	$f^0(x)$	T	Δt
SW	$u_{\mathrm{SW}}(t,x;T)$	$f^0_{\mathrm{hump}}(x;\bar{x})$ with $\bar{x}=(0.5,0.7)$	5	0.05
RB	$u_{\mathrm{RB}}(t,x;T)$	$f^0_{\mathrm{hump}}(x;\bar{x})$ with $\bar{x}=(0.5,0.4)$	3	0.03
NLR	$u_{\mathrm{NLR}}(x)$	$x_2 - \frac{1}{2}$	50	0.5

From the convergence curves shown in Figures 1 to 4 we can draw the following observations:

- Overall, the two approaches (LTP/QTP and L/Q-FBL) reach similar accuracies, as there are no striking differences in the global behavior of the top and bottom curves in Figures 1 to 3.
- A look at the cpu numbers displayed in parenthesis, however, provides a important assessment: whereas the computational cost of the second order QTP scheme increases dramatically for growing remapping periods (which is caused by the stretching of the particle supports), for Q-FBL scheme it remains virtually equal to that of the first order methods (LTP and L-FBL). Thus the main objective of the new scheme is achieved.
- The theoretical gain of one convergence order of the FBL method noticed in Remarks 4.2 and 4.4 is better seen in Figure 4 where the errors are measured in the less stringent L^2. By increasing the remapping period one observes that the accuracy of the LTP simulations deteriorate from second to first order, whereas that of the L-FBL ones remain essentially of second order.

5.2. **Application to the 1D1V Vlasov-Poisson system**

In this section and the following one, we show some preliminary results obtained by applying our Forward-Backward Lagrangian approximation method to a couple of non-linear problems. As we aim at a minimal amount of modifications to existing particle codes, here we only use the FBL reconstruction formula (3.5) to re-initialize the particles with a given remapping frequency, in the spirit of (3.13). Specifically, we consider a 1D1V Vlasov-Poisson system

$$\begin{cases} \{\partial_t + v\partial_x + E(x,t)\partial_v\}\, f(t,x,v) = 0 \\ \partial_x E(t,x) = \displaystyle\int_{\mathbb{R}} f(t,x,v)\,\mathrm{d}v - n_b \end{cases} \qquad (x,v) \in \mathbb{R}^2, \tag{5.2}$$

which models the evolution of a normalized plasma of charged particles in a uniform neutralizing background cloud of density n_b.

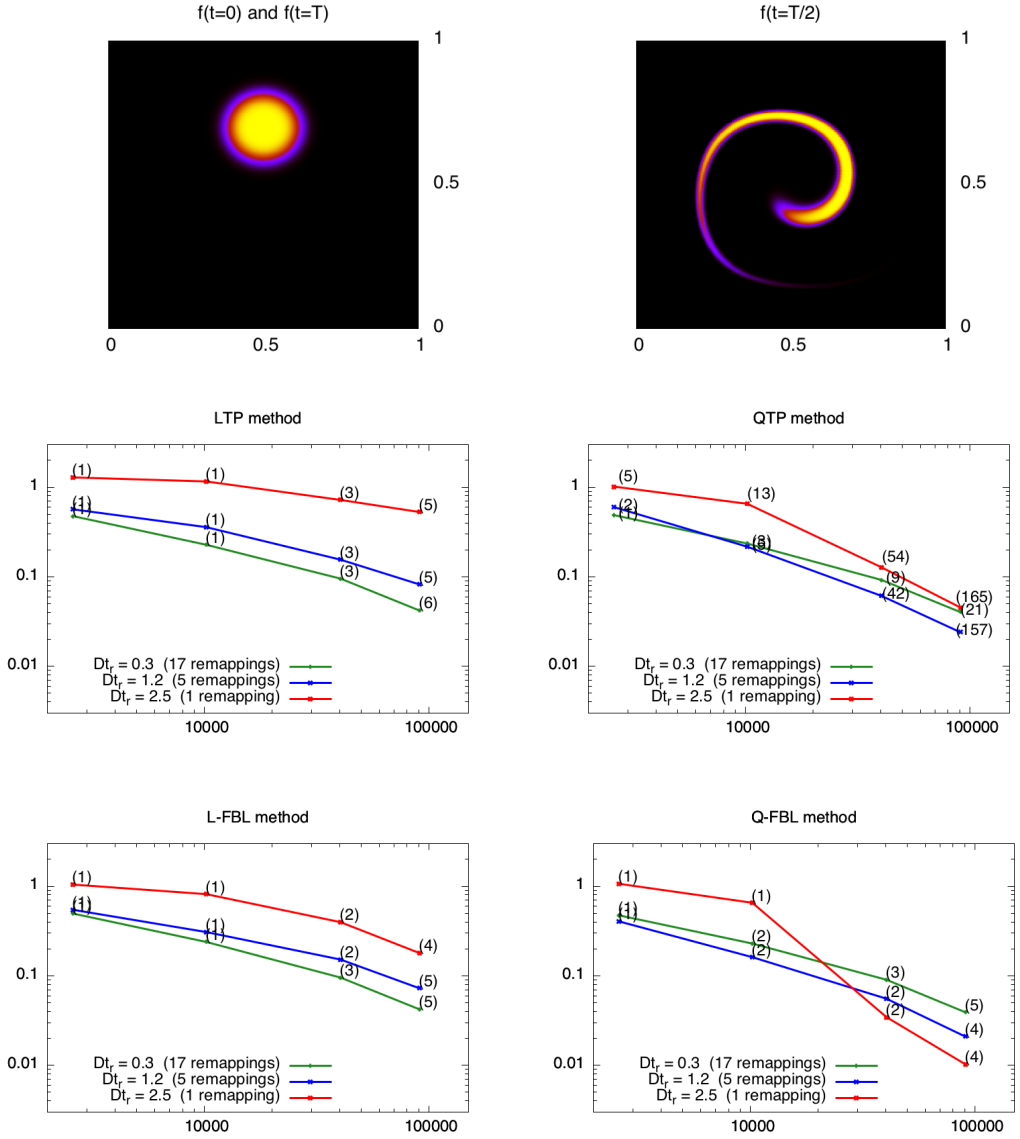

FIGURE 1. (Color) Convergence curves (relative L^∞ errors at $t = T$ vs. number of particles) for the reversible SW test case defined in Table 1, solved with different methods as stated (see text for details). Numbers in parenthesis indicate the approximate cpu times for these runs, including the remappings and final vizualisations. The first row shows the profile of the exact solution: the initial (and final) density $f^0 = f(T)$ is on the left, whereas the intermediate solution $f(T/2)$ (with maximum stretching) is on the right.

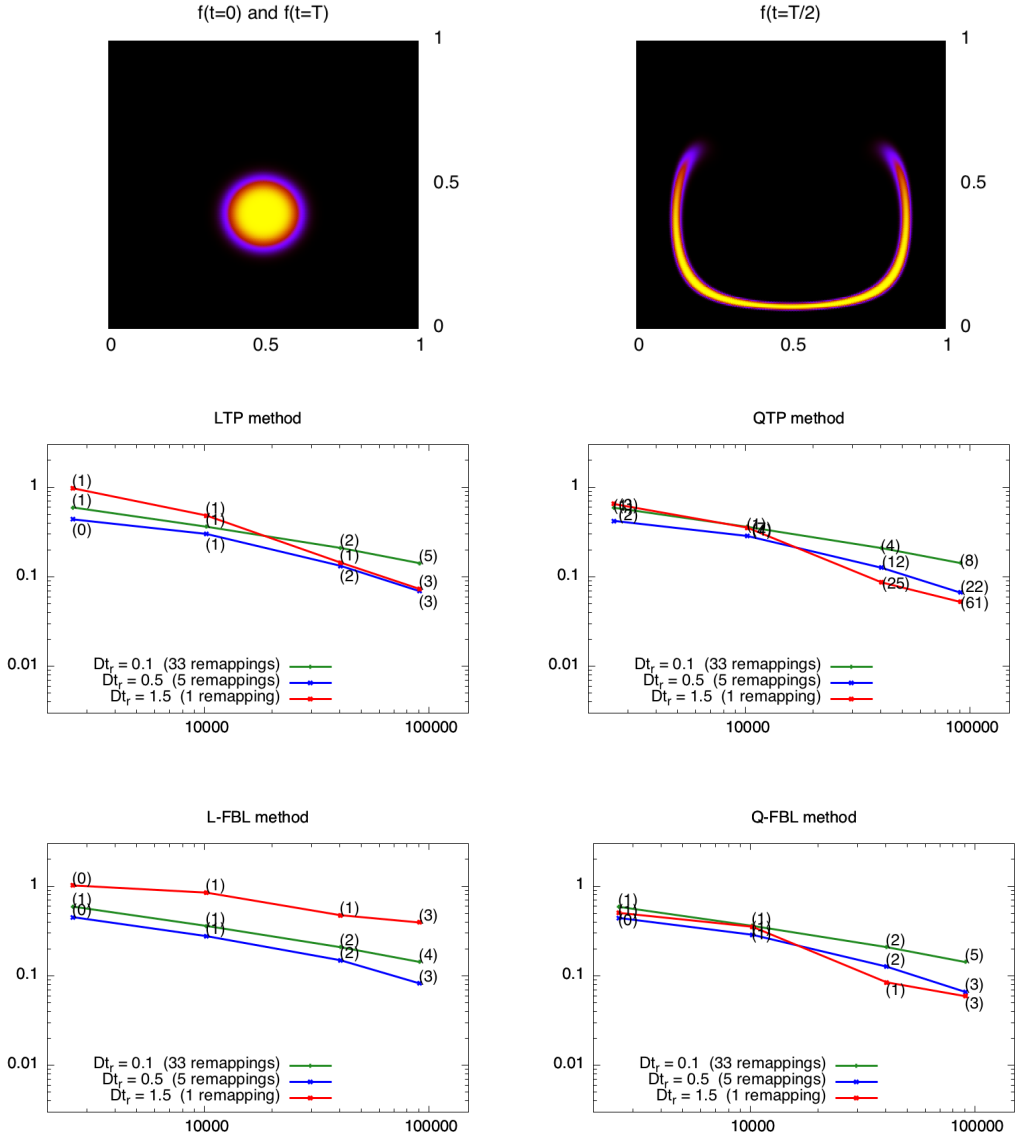

Figure 2. (Color) Convergence curves (relative L^∞ errors at $t = T$ vs. number of particles) for the reversible RB test case defined in Table 1, solved with different methods as stated (see text for details). Numbers in parenthesis indicate the approximate cpu times for these runs, including the remappings and final vizualisations. The first row shows the profile of the exact solution: the initial (and final) density $f^0 = f(T)$ is on the left, whereas the intermediate solution $f(T/2)$ (with maximum stretching) is on the right.

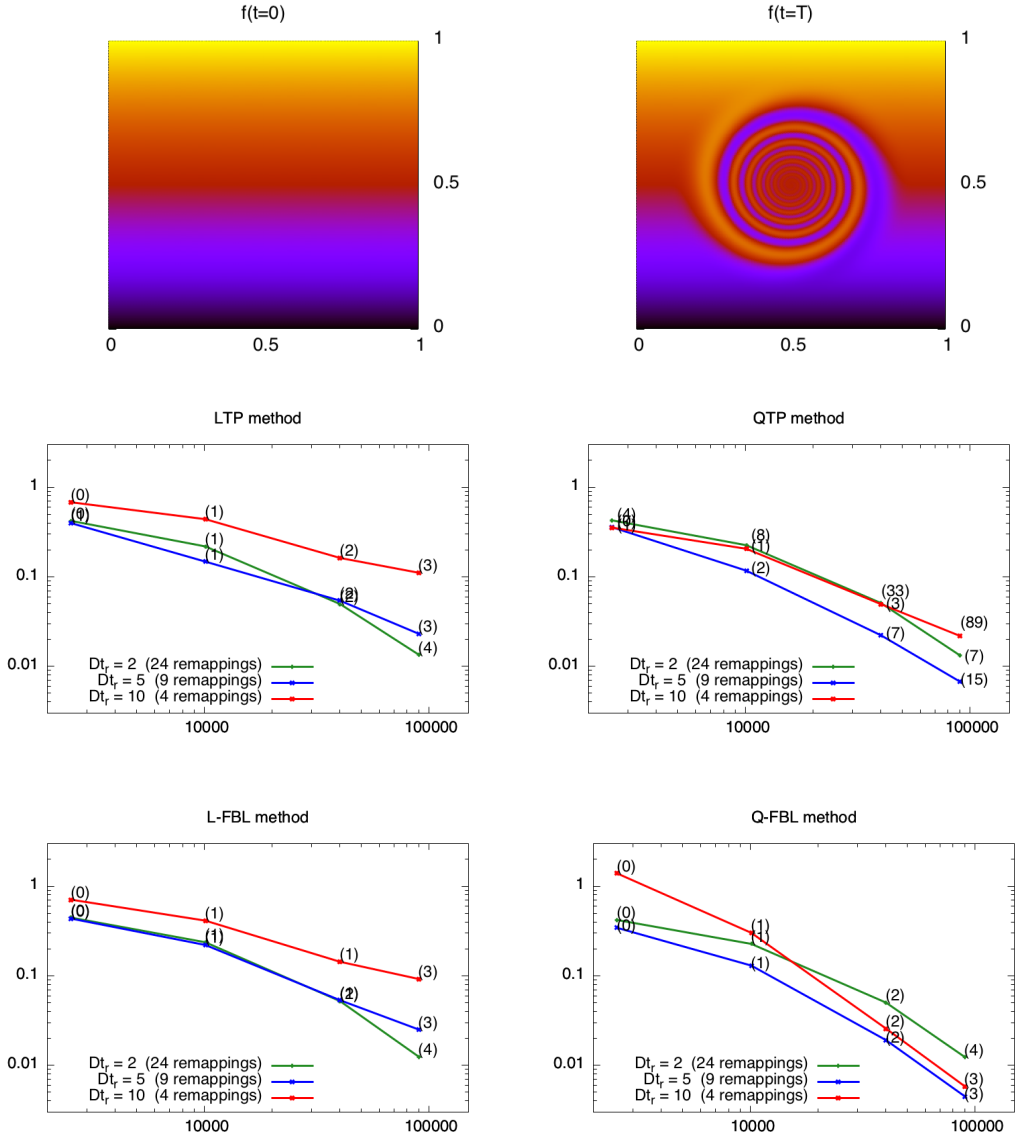

FIGURE 3. (Color) Convergence curves (relative L^∞ errors at $t = T$ vs. number of particles) for the NLR test case defined in Table 1, solved with different methods as stated (see text for details). Numbers in parenthesis indicate the approximate cpu times for these runs, including the remappings and final vizualisations. The first row shows the profile of the exact solution: the initial density $f^0 = f(T)$ is on the left and the final one $f(T)$ is on the right. In this test case the final solution is different than the initial one, but an exact formula based on the backward flow (5.1) is available to estimate the approximation errors.

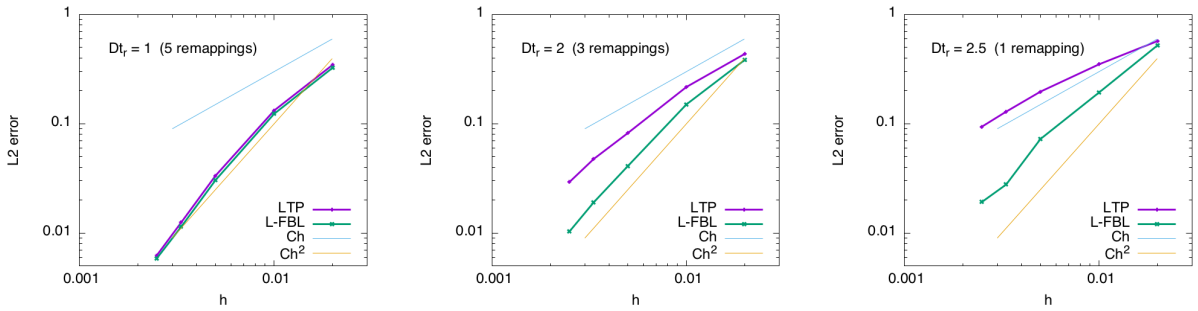

FIGURE 4. (Color) Convergence curves (relative L^2 errors at $t = T$ vs. h) for the reversible SW test case defined in Table 1, solved by the first order LTP and the L-FBL methods. Here the gain of one convergence order appears rather clearly when the remapping period is increased.

To compute numerical approximations to the electric field E and the associated particle trajectories, we employ a standard particle-in-cell (PIC) method [20] which only sees point particles through the piecewise affine shape functions attached to the finite-difference 1D grid used for the field. On the remapping steps we then compute new particles using a cubic spline approximation to the FBL representation of the transported phase-space density f as in (3.8).

To assess our method we use the standard "weak" two-stream instability test-case [18, 28, 10] which initial distribution reads

$$f^0(x,v) = \frac{2(1+5v^2)}{7\sqrt{2\pi}} e^{-\frac{v^2}{2}} \left(1 + A\left(\frac{\cos(2kx)+\cos(3kx)}{1.2} + \cos(kx)\right)\right)$$

with $k = \frac{1}{2}$ and a weak amplitude $A = 0.01$ for the perturbation. This test case is known to develop very thin filaments in the phase space that are difficult to resolve numerically.

In Figure 5 we compare the results of simulations where the particles have been pushed with a standard PIC method as described above, and remapped using either the first order LTP or the first order FBL reconstruction for the transported densities. The approximated densities are shown at $t = 53$ and the remapping period is always set to $\Delta t_R = 3$, which amounts to remapping every 15 time steps, which seemed to be a good value for virtually every run here. The simulations shown on the first line use a grid of 128×128 particles, whereas those on the second line use 512×512 particles. Again, the results show a similar accuracy for both methods, but the cpu times indicate that the FBL is less expensive (16 s. versus 10 s. for the high-resolution runs) due to the enhanced locality of the density reconstructions. We predict that in higher dimensions the gain will be much more significant.

5.3. **Application to the 2D Euler equation**

We then consider the inviscid evolution of an elliptical vortex of compact support. The 2D incompressible Euler equations in vorticity-velocity form write:

$$\begin{aligned} \frac{\partial w}{\partial t} + u \cdot \nabla w &= 0, \\ \nabla \times u &= w, \\ \nabla \cdot u &= 0, \\ \lim_{|x|\to+\infty} |u| &= 0, \end{aligned} \tag{5.3}$$

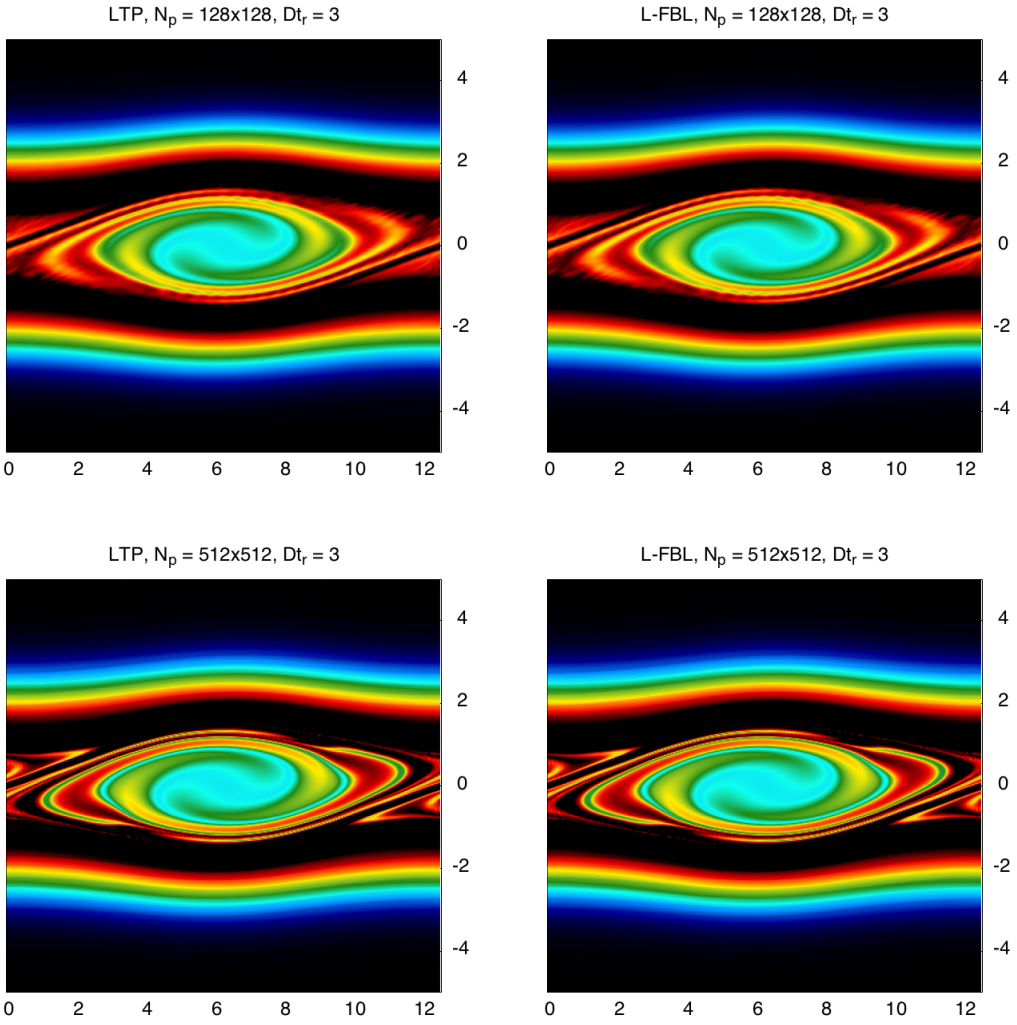

FIGURE 5. Vlasov-Poisson simulations of the two-stream instability described in Section 5.2. The approximated densities shown here have been computed up to $t = 53$ with a standard PIC scheme using 128×128 or 512×512 particles as indicated. On the left plots the particles are periodically remapped using an LTP reconstruction of the density, whereas on the right plots an L-FBL reconstruction is used. The approximated CPU times are close to 3 s. for the low-resolution runs (top row), 16 s. for the high resolution LTP run and 10 s. for the high resolution L-FBL run.

and for the initial condition we take (like in [23] and [4])

$$w^0(x) = w_I^0(\sqrt{(x_1/0.8)^2 + (x_2/1.6)^2}), \qquad w_I^0(r) = 20(1 - \exp(-(2.56085/r)\exp(1/(r-1)))). \quad (5.4)$$

Here the vorticity w plays the role of a transported density and is approximated by a particle representation. The velocity field can be related to w using a Green's function formulation (see [15])

$$u = K * w \qquad \text{where} \qquad K(x) = \frac{1}{2\pi|x|^2}(-x_2, x_1). \quad (5.5)$$

This example has been used as a test case in [23] and in [4] to investigate Smooth Particle (Vortex) methods using adaptive and multilevel remapping techniques.

As we did for the Vlasov-Poisson system, we study here the combination of a standard method to push forward the particle centers and an accurate representation of the density (either with an LTP (2.1)-(2.3) or an FBL (3.5) reconstruction) to re-initialize the particles positions and weights at a given remapping frequency. Since a particle representation of the vorticity w with Dirac masses leads to a velocity field that is singular on particles, it is classical to use a regularization $K_\varepsilon = K * \zeta_\varepsilon$ of the kernel K, with ζ_ε a smooth approximation of the Dirac mass. One can also consider an approximation of the vorticity with smoothed particles, that is

$$w_{h,\varepsilon}(t,x) = \sum_k \omega_k \zeta_\varepsilon(x - x_k(t)),$$

and use it directly in (5.5). In both cases, it leads to the regularized expression of the velocity of the k-th particle

$$u_{h,\varepsilon}(t, x_k(t)) = \sum_j \omega_j K_\varepsilon(x_k(t) - x_j(t)). \tag{5.6}$$

Some examples of smoothing functions ζ_ε and resulting kernels K_ε can be found in [19] and [15].

In Figure 6 we compare numerical vorticities obtained remapped with the first order LTP and FBL reconstructions. We see that the FBL method achieves an improved precision when the remapping period increases, which is reminiscent of the behavior already observed in Figure 4 for the Vlasov-Poisson simulations. Here the simulations involve grids of 50×50 particles corresponding to an average inter-particle distance of $h = 0.08$. In theses simulations the particle trajectories have been computed by applying an RK4 scheme with time step $\Delta t = 0.01$ to the above approximation (5.6) for the velocity, and for the smoothing of the kernel K we have set $\varepsilon = 0.01$. We note that this smoothing scale is much smaller than the inter-particle distance h, which is not sufficient to guarantee the convergence of the reconstructed vorticity in view of the classical analysis [19, 3, 29]. The qualitatively good results displayed in Figure 6 are thus a practical evidence of the beneficial influence of the accurate LTP and FBL reconstructions involved in the remappings.

6. **Conclusion**

In this article we have introduced a novel method to represent the solution of a transport equation using an existing distribution of markers pushed forward. In standard smooth particle methods, the density is reconstructed as a sum of weighted shape functions centered on the markers positions. In the LTP and QTP methods recently developped by the authors, and in other similar methods proposed in the literature, the shapes of the particles are transformed according to a local expansion of the backward flow around each particle. These methods allow to obtain strong convergence properties, but at the price of stretching the particles supports which leads to a loss of locality.

In the Forward-Backward Lagrangian (FBL) method proposed here, the locality is regained by adopting a Lagrangian point of view to reconstruct the solution, which relies on an accurate representation of the initial density (or some reconstructed density at a the last remapping time) and on a global approximation of the backward flow. The latter is obtained by smoothly patching together local expansions of the flow with explicit formulas given in the appendix, around particles seen as (unweighted) flow markers.

Our a priori error analysis shows improved convergence rates for the resulting FBL reconstructions, compared with both standard smooth particles and LTP/QTP methods. Using first order (linear) flow expansions the L-FBL densities converge in $\mathcal{O}(h^2)$, and with second order (quadratic) expansions the Q-FBL densities converge like $\mathcal{O}(h^3)$, which represents a gain of one order compared to the LTP and

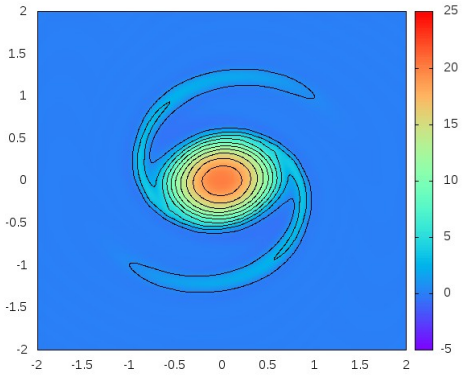

LTP method, $\Delta t_R = 0.1$

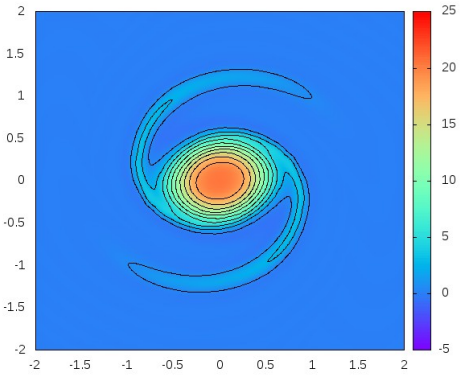

L-FBL method, $\Delta t_R = 0.1$

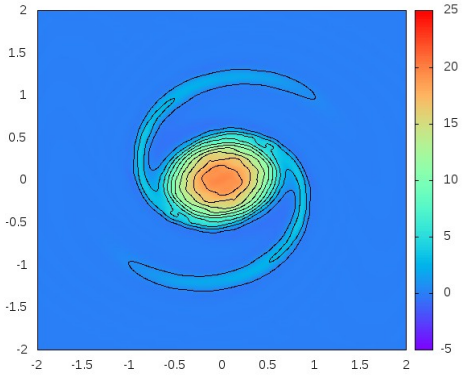

LTP method, $\Delta t_R = 0.15$

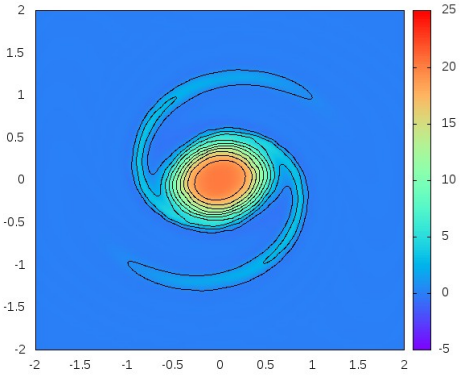

L-FBL method, $\Delta t_R = 0.15$

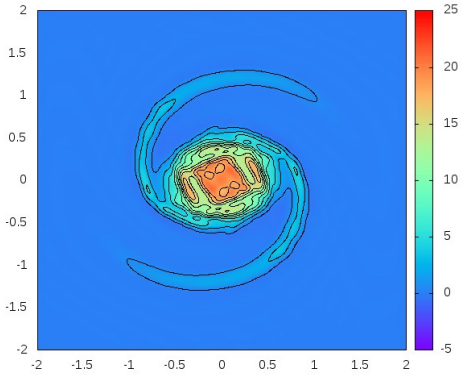

LTP method, $\Delta t_R = 0.2$

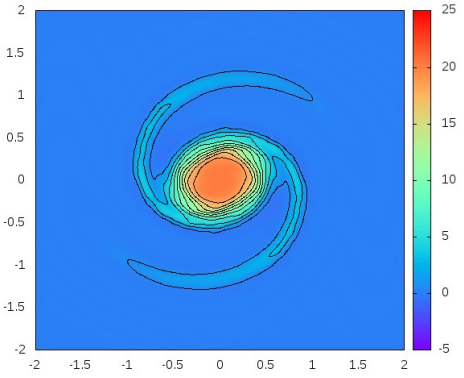

L-FBL method, $\Delta t_R = 0.2$

FIGURE 6. Vorticity contours for equation (5.3)-(5.4) with LTP or L-FBL scheme at time $t = 1.5$, using remapping periods Δt_R as indicated and with particles remapped on a 50×50 grid.

QTP methods. Moreover, the smothness of the FBL densities is stable in $W^{q,\infty}$ norms, with $q \leq 1$ for L-FBL and $q \leq 2$ for Q-FBL.

At the numerical level it is possible to observe the improved accuracy of the FBL reconstructions compared to the LTP ones, especially for increasing remapping periods, however in several practical cases our convergence studies show that the overall quality of both methods is similar. From a CPU time point of view the LTP and L-FBL methods are quite comparable in two dimensions; but due to its good locality the Q-FBL method is much more efficient than the QTP one. Because of the stretching of particle supports the latter has indeed a large computational cost compared to first order methods when the remapping period increases, which has not been observed with the Q-FBL method.

Additional results provided for non-linear problems such as the 1D1V Vlasov-Poisson system or the 2D Euler equation in vorticity form highlight two attractive features of the proposed approach compared to previous ones: On the one hand, its relative efficiency in terms of CPU time when the number of particles increases; and on the other hand its relative accuracy when the remapping period increases. These encouraging results call for more advanced comparisons with existing reconstruction methods. They will be the subject of future articles, in particular for higher dimensional Vlasov-Poisson codes currently under implementation.

Appendix A. Explicit approximation of the flow Jacobian from the particles

Using particles originally distributed on a cartesian grid, i.e., $x_k^0 = hk$, $k \in \mathbb{Z}^d$, we compute the deformation matrices D_k^n approximating the Jacobian matrices of the backward flow at the particles positions (2.2), namely

$$J_{B_{\rm ex}^{0,n}}(x_k^n) = \left(\partial_j (B_{\rm ex}^{0,n})_i (x_k^n)\right)_{1\leq i,j\leq d},$$

as follows. We first approximate the derivatives of the forward flow $F_{\rm ex}^{0,n}$ by finite differences involving the current particle positions $x_k^n = F_{\rm ex}^{0,n}(x_k^0)$. With a centered formula we define

$$J_k^n := \left(\frac{(x_{k+e_j}^n - x_{k-e_j}^n)_i}{2h} \right)_{1\leq i,j\leq d} \approx J_{F_{\rm ex}^{0,n}}(x_k^0) \tag{A.1}$$

and using the relation

$$J_{B_{\rm ex}^{0,n}}(x_k^n) J_{F_{\rm ex}^{0,n}}(x_k^0) = I_d \tag{A.2}$$

which follows by differentiating the identity $x = B_{\rm ex}^{0,n}(F_{\rm ex}^{0,n}(x))$ at x_k^0, we approximate $J_{B_{\rm ex}^{0,n}}(x_k^n)$ with

$$D_k^n := (J_k^n)^{-1}. \tag{A.3}$$

Since we consider a measure-preserving exact flow, we have $\det(J_{F_{\rm ex}^{0,n}}) = 1$ on $\mathbb{R}^d$ and it is reasonable to assume that the $d \times d$ matrix J_k^n is invertible. In the following Lemma we establish a sufficient condition for this, together with some a priori estimates for the resulting approximations.

Lemma A.1. *The approximate forward Jacobian satisfies the a priori estimates*

$$\|J_k^n - J_{F_{\rm ex}^{0,n}}(x_k^0)\|_\infty \leq h^q \frac{|F_{\rm ex}^{0,n}|_{q+1}}{(q+1)!}, \quad q \in \{1,2\} \tag{A.4}$$

and the determinant error is bounded as

$$|\det(J_k^n) - 1| \leq \gamma^n(h) \quad \text{with} \quad \gamma^n(h) = 3d^2 |F_{\rm ex}^{0,n}|_1 \min_{q\in\{1,2\}} \left(h^q \frac{|F_{\rm ex}^{0,n}|_{q+1}}{(q+1)!} \right) \tag{A.5}$$

In particular, if h satisfies

$$h \leq h^*(F_{\rm ex}^{0,n}) := \max_{q\in\{1,2\}} \left(\frac{1}{2} 3d^2 |F_{\rm ex}^{0,n}|_1 \frac{|F_{\rm ex}^{0,n}|_{q+1}}{(q+1)!} \right)^{-\frac{1}{q}} \tag{A.6}$$

then $\det(J_k^n) \geq \frac{1}{2}$ *so that* D_k^n *is well defined, and we have the a priori estimate*

$$\|D_k^n - J_{B_{\rm ex}^{0,n}}(x_k^n)\|_\infty \leq \min_{q\in\{1,2\}} \Big(h^q \frac{|F_{\rm ex}^{0,n}|_{q+1}}{(q+1)!}\Big) 2d^2 |F_{\rm ex}^{0,n}|_1^{2(d-1)}. \tag{A.7}$$

Proof. For conciseness, we denote in this proof

$$J_k^{n,\rm ex} = J_{F_{\rm ex}^{0,n}}(x_k^0) \quad \text{and} \quad D_k^{n,\rm ex} = J_{B_{\rm ex}^{0,n}}(x_k^n)$$

and using the semi-norms (1.8) we observe that

$$\max(\|J_k^{n,\rm ex}\|_\infty, \|J_k^n\|_\infty) \leq |F_{\rm ex}^{0,n}|_1. \tag{A.8}$$

Next we write two Taylor formulas for $s \mapsto F_{\rm ex}^{0,n}(x_k^0 + se_j)$ with $j = 1, \dots, d$, namely

$$F_{\rm ex}^{0,n}(x_k^0 + \sigma h e_j) = F_{\rm ex}^{0,n}(x_k^0) + \sigma h \partial_j F_{\rm ex}^{0,n}(x_k^0) + \int_0^{\sigma h} (\sigma h - s) \partial_j^2 F_{\rm ex}^{0,n}(x_k^0 + se_j)\, {\rm d}s, \quad \sigma = \pm 1 \tag{A.9}$$

and by taking their difference we obtain

$$(2h)^{-1}[F_{\rm ex}^{0,n}]_{x_k^0 - he_j}^{x_k^0 + he_j} = \partial_j F_{\rm ex}^{0,n}(x_k^0) + (2h)^{-1} \int_0^h (h-s)\big(\partial_j^2 F_{\rm ex}^{0,n}(x_k^0 + se_j) - \partial_j^2 F_{\rm ex}^{0,n}(x_k^0 - se_j)\big)\, {\rm d}s.$$

This gives

$$\|J_k^n - J_k^{n,\rm ex}\|_\infty \leq h \frac{|F_{\rm ex}^{0,n}|_2}{2} \tag{A.10}$$

and also

$$\|J_k^n - J_k^{n,\rm ex}\|_\infty \leq h^2 \frac{|F_{\rm ex}^{0,n}|_3}{6} \tag{A.11}$$

which shows (A.4). Using next $\det(J_k^{n,\rm ex}) = 1$ and the Lemma A.2, we find

$$|\det(J_k^n) - 1| \leq d\|J_k^n - J_k^{n,\rm ex}\|_2 (\|J_k^n - J_k^{n,\rm ex}\|_2 + \|J_k^{n,\rm ex}\|_2) \leq 3d^2 |F_{\rm ex}^{0,n}|_1 \min_{q\in\{1,2\}} \Big(h^q \frac{|F_{\rm ex}^{0,n}|_{q+1}}{(q+1)!}\Big) \tag{A.12}$$

since $\|M\|_2 \leq \sqrt{d}\|M\|_\infty$ for $M \in \mathcal{M}_d(\mathbb{R})$. Here the upper bound corresponds to $\gamma^n(h)$, which shows (A.5). From now on we assume that h is as in (A.6), so that $\gamma^n(h) \leq 1/2$, $\det(J_k^n) \geq 1/2$ and D_k^n is well defined. Using the formula $A^{-1} = \det(A)^{-1} C(A)^t$ involving the cofactor matrix $C(A)$ we then write, with $A = D_k^n = (J_k^n)^{-1}$,

$$\|D_k^n\|_\infty \leq d \frac{\|J_k^n\|_\infty^{d-1}}{\det(J_k^n)} \leq d(1 - \gamma^n(h))^{-1} |F^{0,n}|_1^{d-1}. \tag{A.13}$$

With $A = D_k^{n,\rm ex} := (J_k^{n,\rm ex})^{-1}$, see (A.2), this also gives

$$\|D_k^{n,\rm ex}\|_\infty \leq d \frac{\|J_k^{n,\rm ex}\|_\infty^{d-1}}{\det(J_k^{n,\rm ex})} \leq d |F^{0,n}|_1^{d-1}. \tag{A.14}$$

In particular, writing $D_k^n - D_k^{n,\rm ex} = D_k^n (J_k^{n,\rm ex} - J_k^n) D_k^{n,\rm ex}$ gives

$$\|D_k^n - D_k^{n,\rm ex}\|_\infty \leq \|D_k^n\|_\infty \|J_k^n - J_k^{n,\rm ex}\|_\infty \|D_k^{n,\rm ex}\|_\infty \leq h \frac{d^2}{2} (1 - \gamma^n(h))^{-1} |F^{0,n}|_1^{2(d-1)} |F^{0,n}|_2.$$

using the 2nd order estimate (A.10), while the third order estimate (A.11) leads to

$$\|D_k^n - D_k^{n,\rm ex}\|_\infty \leq \|D_k^n\|_\infty \|J_k^n - J_k^{n,\rm ex}\|_\infty \|D_k^{n,\rm ex}\|_\infty \leq h^2 \frac{d^2}{6} (1 - \gamma^n(h))^{-1} |F^{0,n}|_1^{2(d-1)} |F^{0,n}|_3.$$

This ends the proof. ∎

Lemma A.2. *For all* A, $B \in \mathcal{M}_d(\mathbb{C})$ *we have*

$$|\det(A) - \det(B)| \leq d\big[\|A - B\|_2 + \|B\|_2\big] \|A - B\|_2$$

where

Proof. Let $\phi : t \mapsto tA + (1-t)B$. Using that the differential of the determinant is given by

$$D\det(M)H = \mathrm{Tr}(M^* H)$$

we can write

$$\begin{aligned}
|\det(A) - \det(B)| &= |\det(\phi(1)) - \det(\phi(0))| \\
&= \mathrm{Tr}\left(\phi(\theta)^*(A-B)\right), \qquad \text{with } \theta \in]0,1[\\
&= \theta\,\mathrm{Tr}((A-B)^*(A-B)) + \frac{1}{2}\mathrm{Tr}((A-B)^*B + B^*(A-B)) \\
&\le \theta\, d\varrho\left((A-B)^*(A-B)\right) + \frac{d}{2}\varrho\left((A-B)^*B + B^*(A-B)\right) \\
&\le \theta\, d\|A-B\|_2^2 + \frac{d}{2}\|(A-B)^*B + B^*(A-B)\|_2^2 \\
&\le\ d\|A-B\|_2^2 + d\|A-B\|_2\|B\|_2,
\end{aligned}$$

where $\varrho(M)$ is the spectral radius of a matrix M. ∎

Appendix B. Explicit approximation of the flow Hessian from the particles

To compute the quadratic deformation matrices $Q^n_{k,i}$ which approximate the Hessian matrices of the backward flow at the particles positions (2.4), namely

$$H_{(B^{0,n}_{\mathrm{ex}})_i}(x^n_k) = \left(\partial_{j_1}\partial_{j_2}(B^{0,n}_{\mathrm{ex}})_i(x^n_k)\right)_{1\le j_1,j_2\le d}, \qquad 1 \le i \le d,$$

we follow the same principle as for the Jacobian matrices. First, using the current particles positions $x^n_k = F^{0,n}_{\mathrm{ex}}(x^0_k)$ we define approximate forward Hessian matrices as

$$H^n_{k,i} := \Big((h)^{-2}\sum_{\alpha_1,\alpha_2=0}^{1}(-1)^{\alpha_1+\alpha_2}\big(x^n_{k+\alpha_1 e_{j_1}+\alpha_2 e_{j_2}}\big)_i\Big)_{1\le j_1,j_2\le d} \approx H_{(F^{0,n}_{\mathrm{ex}})_i}(x^0_k) \tag{B.1}$$

which corresponds to finite differences on the original grid nodes $x^0_k = hk$, $k \in \mathbb{Z}^d$. Then, differentiating twice the identity $x = I(x) = B^{0,n}_{\mathrm{ex}}(F^{0,n}_{\mathrm{ex}}(x))$ we obtain

$$\left.\begin{aligned}
0 = \partial_{j_1}\partial_{j_2}(I)_i(x) = \sum_{l_1,l_2=1}^{d}\partial_{l_1}\partial_{l_2}(B^{0,n}_{\mathrm{ex}})_i(F^{0,n}_{\mathrm{ex}}(x))\partial_{j_1}(F^{0,n}_{\mathrm{ex}})_{l_1}(x)\partial_{j_2}(F^{0,n}_{\mathrm{ex}})_{l_2}(x) \\
+\sum_{l=1}^{d}\partial_l(B^{0,n}_{\mathrm{ex}})_i(F^{0,n}_{\mathrm{ex}}(x))\partial_{j_1}\partial_{j_2}(F^{0,n}_{\mathrm{ex}})_l(x)
\end{aligned}\right\} \quad \begin{array}{c}\text{for} \\ 1\le i,j_1,j_2\le d.\end{array}$$

At $x = x^0_k$ and denoting for conciseness the exact Hessian matrices by

$$H^{n,\mathrm{ex}}_{k,i} = H_{(F^{0,n}_{\mathrm{ex}})_i}(x^0_k) \quad \text{ and } \quad Q^{n,\mathrm{ex}}_{k,i} = H_{(B^{0,n}_{\mathrm{ex}})_i}(x^n_k), \qquad 1 \le i \le d, \tag{B.2}$$

this gives $0 = (J^{n,\mathrm{ex}}_k)^t Q^{n,\mathrm{ex}}_{k,i} J^{n,\mathrm{ex}}_k + \sum_{l=1}^d (D^{n,\mathrm{ex}}_k)_l H^{n,\mathrm{ex}}_{k,l}$, hence with (A.2),

$$Q^{n,\mathrm{ex}}_{k,i} = -(D^{n,\mathrm{ex}}_k)^t\Big(\sum_{l=1}^{d}(D^{n,\mathrm{ex}}_k)_{i,l}H^{n,\mathrm{ex}}_{k,l}\Big)D^{n,\mathrm{ex}}_k. \tag{B.3}$$

For the approximate backward Hessian matrix at x_k^n we thus set

$$Q_{k,i}^n := -(D_k^n)^t \Big(\sum_{l=1}^d (D_k^n)_{i,l} H_{k,l}^n \Big) D_k^n \tag{B.4}$$

where the approximate backward Jacobian matrix D_k^n is computed as in Appendix A.

Lemma B.1. *The forward Hessian matrices $(H_k^n)_i$ defined above satisfy the a priori estimates*

$$\|H_{k,i}^n - H_{(F_{\rm ex}^{0,n})_i}(x_k^0)\|_\infty \le C |F_{\rm ex}^{0,n}|_{W^{3,\infty}} h \tag{B.5}$$

with a constant C that depends only on the dimension d. Moreover if $h \le h^*(F_{\rm ex}^{0,n})$ as in (A.6)*, the backward ones $Q_{k,i}^n$ satisfy*

$$\|Q_{k,i}^n - H_{(B_{\rm ex}^{0,n})_i}(x_k^n)\|_\infty \le C_Q(F_{\rm ex}^{0,n}) h \tag{B.6}$$

with a constant $C_Q(F_{\rm ex}^{0,n})$ that depends on $|F_{\rm ex}^{0,n}|_{W^{q,\infty}}$ with $1 \le q \le 3$.

Proof. Expressing the finite differences in (B.1) as local averages of second derivatives of $F_{\rm ex}^{0,n}$, one easily verifies the estimate (B.5), as well as the bounds

$$\|H_{k,i}^n\|_\infty \le C |F_{\rm ex}^{0,n}|_{W^{2,\infty}}, \qquad 1 \le i \le d \tag{B.7}$$

also satisfied by the exact $H_{k,i}^{n,\rm ex}$. To show (B.6) it then suffices to use the identities (B.3) and (B.4), together with the estimates (B.5) on H_k^n, (A.7) on D_k^n (with $q = 1$) and the bounds (A.13), (A.14), (B.7) satisfied by the exact and approximate (backward) Jacobian and (forward) Hessian matrices. ■

Acknowledgements

The authors thank Stéphane Colombi for fruitful discussions on the backward flow reconstructions, and Mehdi Badsi who implemented a 2d2v version of the LTPIC method showing the impact of the shape elongations on the performances. They also thank Antoine Le Hyaric who contributed to the implementation of a preliminary 2d2v version of the FBL method in the Selalib library, as well as the Selalib developers for their continued support. This work has been carried out within the framework of the Consortium and has received funding from the Euratom research and training programme 2014-2018 under grant agreement No 633053. The views and opinions expressed herein do not necessarily reflect those of the European Commission.

Bibliography

[1] C. Alard and S. Colombi. A cloudy Vlasov solution. *Monthly Notices of the Royal Astronomical Society*, 359(1):123–163, May 2005.

[2] W.B. Bateson and D.W. Hewett. Grid and Particle Hydrodynamics. *Journal of Computational Physics*, 144:358–378, 1998.

[3] J.T. Beale and A. Majda. Vortex methods. II. Higher order accuracy in two and three dimensions. *Mathematics of Computation*, 39(159):29–52, 1982.

[4] M. Bergdorf, G.-H. Cottet, and P. Koumoutsakos. Multilevel adaptive particle methods for convection-diffusion equations. *Multiscale Modeling & Simulation*, 4(1):328–357, 2005.

[5] M. Bergdorf and P. Koumoutsakos. A Lagrangian particle-wavelet method. *Multiscale Modeling & Simulation*, 5(3):980–995, 2006.

[6] A. Biancalani, A. Bottino, S. Briguglio, A. Koenies, Ph. Lauber, A. Mishchenko, E. Poli, B.D. Scott, and F. Zonca. Linear gyrokinetic particle-in-cell simulations of Alfven instabilities in tokamaks. ⟨arXiv:1510.01945⟩, 2015.

[7] O. Bokanowski, J. Garcke, M. Griebel, and I. Klompmaker. An adaptive sparse grid semi-Lagrangian scheme for first order Hamilton-Jacobi Bellman equations. *Journal of Scientific Computing*, 55(3):575–605, 2013.

[8] M. Campos Pinto. Towards smooth particle methods without smoothing. *Journal of Scientific Computing*, 2014.

[9] M. Campos Pinto and F. Charles. Uniform Convergence of a Linearly Transformed Particle Method for the Vlasov–Poisson System. *SIAM Journal on Numerical Analysis*, 54(1):137–160, January 2016.

[10] M. Campos Pinto, E. Sonnendrücker, A. Friedman, D.P. Grote, and S.M. Lund. Noiseless Vlasov–Poisson simulations with linearly transformed particles. *Journal of Computational Physics*, 275(C):236–256, October 2014.

[11] A. Cohen and B. Perthame. Optimal Approximations of Transport Equations by Particle and Pseudoparticle Methods. *SIAM Journal on Mathematical Analysis*, 32(3):616–636, October 2000.

[12] S. Colombi and C. Alard. A "metric" semi-Lagrangian Vlasov-Poisson solver. Submitted, 2016.

[13] C.J. Cotter, J. Frank, and S. Reich. The remapped particle-mesh semi-Lagrangian advection scheme. *Quarterly Journal of the Royal Meteorological Society*, 133(622):251–260, 2007.

[14] G.-H. Cottet, P. Koumoutsakos, and M.L.O. Salihi. Vortex Methods with Spatially Varying Cores. *Journal of Computational Physics*, 162(1):164–185, July 2000.

[15] G.H. Cottet and P. Koumoutsakos. *Vortex Methods: Theory and Practice*. Cambridge University Press, Cambridge, 2000.

[16] N. Crouseilles, T. Respaud, and E. Sonnendrücker. A forward semi-Lagrangian method for the numerical solution of the Vlasov equation. *Computer Physics Communications*, 180(10):1730–1745, October 2009.

[17] J. Denavit. Numerical Simulation of Plasmas with Periodic Smoothing in Phase Space. *Journal of Computational Physics*, 9:75–98, 1972.

[18] F. Filbet and E. Sonnendrücker. Comparison of Eulerian Vlasov solvers. *Computer Physics Communications*, 150:247–266, 2003.

[19] O.H. Hald. Convergence of Vortex Methods for Euler's Equations. II. *SIAM Journal on Numerical Analysis*, 16(5):726–755, October 1979.

[20] R.W. Hockney and J.W. Eastwood. *Computer simulation using particles*. Taylor & Francis, Inc, Bristol, PA, USA, 1988.

[21] T.Y. Hou. Convergence of a Variable Blob Vortex Method for the Euler and Navier-Stokes Equations. *SIAM Journal on Numerical Analysis*, 27(6):1387–1404, December 1990.

[22] P. Koumoutsakos. Inviscid Axisymmetrization of an Elliptical Vortex. *Journal of Computational Physics*, 138:821–857, December 1997.

[23] P. Koumoutsakos. Inviscid axisymmetrization of an elliptical vortex. *Journal of Computational Physics*, 138(2):821–857, 1997.

[24] R.J. LeVeque. High-resolution conservative algorithms for advection in incompressible flow. *SIAM Journal on Numerical Analysis*, pages 627–665, 1996.

[25] A. Magni and G.-H. Cottet. Accurate, non-oscillatory, remeshing schemes for particle methods. *Journal of Computational Physics*, 231(1):152–172, 2012.

[26] J.J. Monaghan. Extrapolating B. Splines for Interpolation. *Journal of Computational Physics*, 60:253, September 1985.

[27] R.D. Nair, J.S. Scroggs, and F.H.M. Semazzi. A forward-trajectory global semi-Lagrangian transport scheme. *Journal of Computational Physics*, 190(1):275–294, September 2003.

[28] J.-M. Qiu and A. Christlieb. A conservative high order semi-Lagrangian WENO method for the Vlasov equation. *Journal of Computational Physics*, 229:1130–1149, 2010.

[29] P.-A. Raviart. An analysis of particle methods. In *Numerical methods in fluid dynamics (Como, 1983)*, pages 243–324. Lecture Notes in Mathematics, Berlin, 1985.

[30] Selalib. Semi-Lagrangian Library. http://selalib.gforge.inria.fr/.

[31] M. Unser and I. Daubechies. On the approximation power of convolution-based least squares versus interpolation. *Signal Processing, IEEE Transactions on*, 45(7):1697–1711, 1997.

[32] B. Wang, G.H. Miller, and P. Colella. A Particle-In-Cell method with adaptive phase-space remapping for kinetic plasmas. *SIAM Journal on Scientific Computing*, 33:3509–3537, 2011.